LAWRENCE
LIVERMORE
NATIONAL
LABORATORY

LLNL-JRNL-408396

Heterogeneous Directional Mobility in the Early Stages of Polymer Crystallization

N. Lacevic, L. E. Fried, R. H. Gee

November 4, 2008

Journal of Chemical Physics

Disclaimer

Heterogeneous Directional Mobility in the Early Stages of Polymer Crystallization

Naida Lacevic*, Laurence E. Fried, and Richard H. Gee

Chemistry, Materials, and Life Sciences Directorate

Chemical Sciences Division

Lawrence Livermore National Laboratory, P.O. Box 808, L-268, Livermore CA 94550

Abstract

Recently we demonstrated via large-scale molecular dynamics simulations a 'coexistence period' in polymer melt ordering before crystallization, where nucleation and growth mechanisms coexist with a phase-separation mechanism [Nature Mat. **5,** 39-43 (2006)]. Here we present an extension of this work, where we analyze the directional displacements as a measure of the mobility of monomers as they order during crystallization over more than 100 *ns* of simulation time. It is found that the polymer melt, after quenching, rapidly separates into many ordered hexagonal domains separated by amorphous regions, where surprisingly, the magnitude of the monomer's displacement in the ordered state, parallel to the domain axial direction, is similar to its magnitude in the melt. The monomer displacements in the domain's lateral direction are found to decrease during the time of the simulation. The ordered hexagonal domains do not align into uniform lamellar structures during the timescales of our simulations.

* To whom correspondence should be addressed, e-mail: lacevic2@llnl.gov.

Introduction

Polymer crystallization involves complex correlated motion of groups of monomers and polymer chains that pass from an amorphous state to the ordered state. A prime example of correlated motion during crystallization is the polymer's conformational change from random coil to chain folded structures. Yet much remains to be understood regarding the nature of cooperativity, correlated motion and its direct relevance to polymer crystallization. Hoffman, Lauritzen and co-workers'[1] theory of the growth rate of a lamella offered a simple picture of direct chain segment attachment from the polymer melt to the crystalline lamella. The lamellae thickness is then determined via the modified Gibbs-Thomson equation. This simple theory was seriously questioned because of several experimental findings e.g., the observation of mesomorphic hexagonal phase in polyethylene under high pressures by Keller[2] and the "build-up of a precursor phase" before crystallites were observed by Kaji and collaborators.[3] The existence of such a pre-transition state is now well established in experiments,[4,5] theory[6] and computer simulations.[7-9]

An important step in incorporating the existence of the pre-transition state and evolution of subsequent metastable phase in the current theories of polymer crystallization is to understand the polymer motion in systems undergoing such a transition, which is qualitatively different from that experienced by polymers precipitating from the solution (see e.g., Rastogi *et al.*[10]). Furthermore, experiments which track the motion of individual polymer chains are not practical in this regime, so large-scale simulations are excellent candidates to advance our knowledge and provide insight about molecular motion of polymer chains in a dense melt during the early stages of polymer ordering.

In recent years there have been fundamental advances in understanding polymer crystallization from the melt using molecular dynamics simulations. Yamamoto described monomer ordering of undercooled melts of high molecular weight (C_{1000}) chains near a crystalline wall,[11] and Muthukumar and co-workers showed that a long polymer chain can nucleate at several places.[12] However, Muller-Plathe and Meyer were the first to study emerging ordered domains from the melt.[13] Further, Hikosaka *et al.* has established a theory of chain sliding diffusion[14] to aid in the understanding of the molecular mobility in the ordered hexagonal phase upon polymer

crystallization. These pioneering works have provided the foundation necessary for further studies to fully understand the polymer crystallization process.

In order to observe the pre-transition state and monitor polymer dynamic ordering from the melt after the pre-transition in computer simulations, it is necessary to consider significantly larger and denser systems than have been studied before, because the length scale of density fluctuations associated with pre-transition is on the order of 16 *nm*.[15] Further, the molecular motion associated with dense, high molecular weight (entangled) polymer chains in the melt undergoing crystallization is significantly different from polymer chains crystallizing from solution.[10]

In this work we provide insights into the following questions: (1) What is the mechanism and degree of monomer mobility inside the ordered domains? (2) What is the internal structure of the ordered domains during the simulations? (3) Once ordered domains are formed, do the ordered domains align in some preferred direction, or in other words can we monitor the gradual transition of randomly oriented ordered domains and observe their alignment?

Methodology

A. Polymer Model

Our goal is to obtain qualitative features of the dynamics of polymer ordering during and after ordered domain formation, as such we are concerned with capturing the general qualities of linear polymer systems rather than exactly reproducing a specific material such as polyethylene (PE) in which the time scales observed for such processes experimentally are much longer than those accessible via molecular dynamics simulations. Therefore, the force field parameters are modeled after the paper by Paul *et al.*[16] for *n*-alkanes (herein referred to as the PYS model), however, the parameters for the bond torsions are slightly modified in our model to enhance computational efficiency.

The polymer molecules considered in this paper consist of united-atom (UA) monomers that interact with each other via a 12-6 Lennard-Jones (LJ), given by

$$E_{vdW}(r) = 4\varepsilon\left[\left(\frac{\sigma}{r}\right)^{12} - \left(\frac{\sigma}{r}\right)^{6}\right], \qquad r \le r_c(2.5\sigma) \tag{1}$$

where ε = 0.112 kcal/mol and σ = 0.401 *nm*, and *r* is the distance between monomers which are on separate chains or on the same chain separated by three or more bonds. The bonding energy between neighboring monomers on a chain is given by

$$E_{bond} = K_b(r - r_0)^2, \tag{2}$$

where the bond spring constant K_b = 350 kcal/mol and the equilibrium bond length is r_0 = 0.153 *nm*. The angle bending term is given by

$$E_{angle} = K_\theta(\theta - \theta_0)^2, \tag{3}$$

where the angle spring constant $K_\theta = 60$ kcal/mol rad^{-2} and the equilibrium angle is θ_0 = 109°. The torsional term is given by

$$E_{torsion} = \sum_{n=1}^{3} K_n\left[1 - \cos(n\phi - \phi_n)\right], \tag{4}$$

where K_1 = 0.81 kcal/mol, ϕ_1 = 0°, K_2 = -0.43 kcal/mol, ϕ_2 = 180°, K_3 = 1.62 kcal/mol, ϕ_3 = 0°.

The modification to the bond torsional potential has the effect of changing the energy difference between *gauche* and *trans* conformational states, as well as raising the *trans* to *gauche* energy barrier as compared to the bond torsional potential of Paul *et al.*,[16] thus, the chain torsional stiffness is somewhat higher, enhancing computational efficiency. Similar modifications have been reported in computer simulation studies of polyethylene,[17] and similar energy differences are obtain for other linear polymers, such as polytertafluoroethylene.[18]

The modification to the torsional potential enhances ordering at computationally accessible timescales. For comparison, we performed simulations on bulk PE melts using the *n*-alkane

polymer model of Paul *et al.*[16] on an ensemble composed of 64 polymer chains of 768 methylene (CH_2) united-atom (UA) 'monomers' per chain, and found that well defined ordered domains develop within ~200 *ns* at 280 *K*, therefore, the multi-million atom systems necessary for this study (required to capture the appropriate length scales of ordered domains) would be computationally impractical. The consequences of such modifications to the torsional potential of polymers have been investigated in the past by Gee and Boyd.[19]

Figure 1 shows the bond torsional potentials and conformational populations of the model polymer used in this work along with the polymer model of Paul *et al.*[16] at 500 K. It is evident that the polymer model used in this work has a larger *trans* fraction, as compared to the PYS model due to the larger *gauche/trans* energy difference.

In summary this potential shares similarity with other united atom potentials[12,13,20] capable of observing crystallization at timescales accessible via molecular dynamics simulations.

B. Initial ensemble preparation and simulations details

The multi-million C_{768} melt ensemble used in this work was taken from our previous work,[8] in constant temperature and pressure (*NPT*) MD simulations were previously performed for equilibration. Specifically, the polymer melt was initially simulated at 600 K, where the initial starting polymer configurations of the amorphous melt structures were generated by assigning random values to all rotatable torsions in the polymer chain using a Monte Carlo method. The resulting amorphous structure was then relaxed by energy minimization. The periodic structure was allowed to relax under *NPT* conditions for a minimum of 5 *ns* at a pressure of 0 Pa. Following this step, the melts were cooled in *NPT* runs in increments of 50 K and equilibrated for a minimum of 5 *ns* each at the desired temperature (600 K, 550 K, and 500 K). When cooled to a temperature of 450 K, the polymer melt was found to undergo ordering (further details of the simulations and of the early stage melt ordering can be found in our previous study Ref. [8]). The work presented here focuses on the polymer mobility and development of the ordered domains up to 100 *ns* of simulation time.

The polymer melt ensemble considered in this work is composed of 5,832 polymer chains, each consisting of 768 UA monomers (4,478,976 CH_2 UA monomers; M_w = 10,752 g/mol). All computations were carried out using the LAMMPS code.[21] The equations of motion were integrated using the Verlet algorithm[22] with a time step of 4 *fs* at the temperature at which polymer ordering occurred (450 K). A Nose-Hoover-type thermostat[23] with a relaxation time of 0.1 *ps* was used to control the temperature, and the pressure was controlled isotropically.[24]

C. Chain's flexibility: Characteristic ratio and persistence length

Since the characteristic ratio, C_n, is sensitive to the energetics of local bond conformations in polymer chains, comparison of the computed values of C_n for our model and experimental values that are available for various flexible polymers is an important metric that quantifies how the modification to the torsional potential described in part A alters the statistical behavior of conformationally disordered polymer chains. We compute the characteristic ratio,

$$C_n = \frac{\langle R^2 \rangle}{nl^2}, \tag{5}$$

and the persistence length,

$$L_P = \frac{l(C_\infty + 1)}{2}, \tag{6}$$

where $\langle R^2 \rangle$ is the mean-square end-to-end distance, n is the number of bonds on a single chains, l is the bond length, and C_∞ is the characteristic ratio for infinitely long chains.[25] At 500 K, C_∞ = 10.7 was computed from our molecular dynamics simulations. We also estimated C_∞ for our model via a three-state Rotational Isomeric State approximation (RIS) using the code from Ref. [26] which yields 12.8 at 500 K. Note that RIS gives C_∞ = 7.4 for PYS model at 500 K. Further, experimental C_∞ values at 413 K for polyethylene range from 6.7 to 7.8 (see Refs. 27 and 28, respectively). The computed persistence length, L_p, for our system is 0.89 *nm* at 500 K. As expected, the polymer chains studied via this model are less flexible than PYS model, but more flexible than many semi-flexible polymers that may have persistence lengths ranging up to 12 *nm* (see e.g., Ref. [29]).

D. Computational Details

All simulations were performed using Livermore Computing machines. Two different machine architectures were used; the first is a cluster of 2048 Intel Xeon 2.4GHz processors (MCR cluster), the second is a cluster of 4096 Intel Itanium2 Tiger4 1.4GHz processors (Thunder cluster). The peak performance of the MCR and Thunder clusters is 11.06 TFlop/s and 22.9 TFlop/s, respectively. We used 1024 (Thunder) or 2048 (MCR) processors. The total simulation time of our polymer simulations were ~100 *ns*, which took ~1.6x10^6 processor hours.

Results and Discussion

We first review the general theoretical framework used to obtain the relevant quantities that will enable us to compute the monomer's directional displacement. Consider a polymer melt of M chains with N monomers on each chain. A chord vector, c_i, is defined as a line segment connecting the midpoints of two adjacent bonds on a polymer chain. The order parameter, $P_c = \left\langle (3\cos^2\theta - 1)/2 \right\rangle_c$, where θ is the angle between two consecutive chord vectors, measures the "straightness" of the chain. A "stem" can then be identified as a straight segment of a chain with direction, $\mathbf{C} = \frac{\sum_i^{N_{chords}} \mathbf{c}_i}{N_{chords}}$, where N_{chords} is the number of chord vectors within a given stem. The average stem length, $\langle l_s(t) \rangle$, and inter-stem alignment, are sensitive to ordering as has been shown in several papers dealing with the simulation of polymer crystallization.[7,8,13,17,30]

Here, stems are defined by comparing the orientation of a chord vector with other chords along the backbone of the chain, which is defined as the 5 chords on the chain on either side of the designated chord. If the average angle between designated chord vectors and the adjacent backbone chord vectors is less then 10°, it is considered ordered. In this manner, each chord vector is assigned a "state", s, of either ordered or disordered, which is designated (1) or (0), respectively, thus generating a sequence of (1)'s and (0)'s along each chain. This 'mapping' is

performed for all chains. To smooth random fluctuations, each designated chord vector state, s_i, in the sequence is further averaged, such that $s_i = 1$ if $\sum_{-5 \le l \le 5} s_i \ge 5.$ and $s_i = 0$ if $\sum_{-5 \le l \le 5} s_i < 5.$

Once stems are found, they are then grouped to form clusters, representing the ordered domains in the system, such that the axis of each stem is aligned within 20° of its neighbors and lines passing through their centers of mass along their axis have minimum separations within 0.5 *nm*. Only clusters containing stems with the minimum length of 15 CH_2 UA monomers (~1.8 *nm*) are retained. Since the algorithm depends on parameters such as alignment angles, stem nearest neighbor distances and number of monomers over which the average chord is calculated, we have explored this parameter space and find that the resulting clusters are relatively robust against small perturbations of the parameters. Note that the minimum stem length of 15 monomers in an ordered domain is large compared to the computed persistence length of the polymer chains. This allows us to monitor the trends in chain mobility that will not be affected by the stiffness of the chains.

Figure 2*a* shows individual stems isolated from a melt (equilibrated at 500 K) at the initial time of the simulation using the criterion explained above. We note that at this time there are no clusters of stems (ordered domains). Once the melt has been allowed to evolve for 2 *ns* at 450 K, hexagonal ordered domains are identified, and the largest 50 ordered domains are shown in Figure 2*b* (amorphous regions are not shown for clarity). This early time ordered domain formation could be viewed as the aforementioned pre-transition as described in Ref. [8]. In this earlier work[8], we demonstrated via the evolution of the structure factor that ordering occurs before the melt densifies (demonstrated by the shift in the Bragg peak), and that this ordering is reminiscent of a process of spinodal decomposition. These ordered domains are found to continue to grow in time, where the 50 largest ordered domains at 100 *ns* are shown in Figure 2*c* and *d* (the largest domain identified at 100 *ns* is found to be more than 60,000 monomers). Figure 2*e* shows both amorphous and ordered regions at 100 *ns*, and demonstrates that there are ordered domains that almost span the entire simulation cell.

To further quantify the chain ordering process, we have calculated basic statistics related to the domain formation. Figure 3*a* shows the average number of ordered domains, N_c, as a function

of time, that consist of stems whose lengths are greater than 15 monomers. It is observed that N_c first increases, reaching a maximum of ~200 domains (in our 1.25x10^{-4} μm^3 simulation cell) which corresponds roughly to the end of the pre-transition (induction period) at ~10 *ns*, and then decreases in time with the merger and ripening of domains. This is a signature of the coalescence of the ordered domains. Figure 3*b* shows the average number of monomers, N_{pc}, in the ordered domains. As expected, N_{pc} increases in time, a further indication of domain coarsening. Figure 3*c* shows the average stem length in the ordered domains, $\langle l_s(t) \rangle$. It increases in time, and is related to the average size (or thickness) of the domains. At late times the average stem length exceeds 5 *nm*.

Figure 3*d* shows a time-dependent correlation function of the domains' axial directions, $<|\mathbf{A}_i \cdot \mathbf{A}_j|>$, which is a measure of domain alignment. The axial direction of a domain is taken as the mean direction of its stems, $\mathbf{A} = <\mathbf{C}> / |<\mathbf{C}>|$. Although the domains grow and coalesce during the simulation, we do not see alignment of their axes on the times scales of the simulations, up to 100 *ns*. In fact, the degree of alignment drops somewhat at early times (5 – 10 *ns*), perhaps partially due to merging of similarly aligned domains, and then saturates, corresponding to an average angle of ~45^o between domain pairs. The overall lack of domain alignment over the course of the simulations may be attributed to the effective physical cross-linking of neighboring domains formed by chains that bridge multiple domains. Consequently, the intra-domain mobility of the chains forming these cross-links will be of great importance to the further micro-scale ordering of the structures.

To better understand the structure of the ordered domains, we project the stems' centers of mass (isolated as described above) onto a plane normal to their domains' axial directions (obtained as an average of all stem directions that belong to that particular domain). We find that the angular distribution of neighboring points coincides well with what we would expect from a hexagonal structure. We conclude that stems pack in a hexagonal domain structure with defects which resembles a sketch of the "mesomorphic" phase of reference[5]. As such, the ordered domains are similar to the "granular domains that later on transform to crystalline granular domains" that Strobl describes.[5] We also note by visual inspection that the structure of the domain is far from

being a perfect crystal. The chains have significant curvature that adds complexity in performing cluster identification. This is also seen in experiments, where the lamella's truncation faces are often curved.[31] We have also investigated the degree to which the straightening and alignment of the chains results in two distinct thermodynamic states. To this end, we have performed energy minimizations of several polymer configurations at various times during ordering, and calculated the contribution of each particle to the non-bonded energy. All atom positions are allowed to relax to their local potential energy minima while the system remains at constant volume and the minimization is performed to eliminate thermally induced fluctuations. We find that of the energy distribution after minimization has a bimodal character indicative of two co-existing thermodynamic states, with the ordered phase having a significantly lower energy than the amorphous state (see Figure 4). Complete details of this investigation will be presented in a future publication.

One of the most surprising results found in these simulations is the large-scale atomic segmental motion (concerted monomer displacement of stems') inside the ordered domains. We compute the displacement for all monomers, $\Delta\mathbf{r}_i(\Delta t)$, over intervals of $\Delta t = 80$ *ps*. Figure 5*a* shows an isolated domain at 50 *ns,* where monomers are colored according their displacements (white and black colored monomers are the sets with the 5% smallest and largest displacements, respectively). Entire stems move in concert due to the constraints imposed by the domain structure, in a process related to "chain sliding diffusion" suggested by Hikosaka,[14,32] and is similar to relaxation processes seen experimentally in PE.[33] Hikosaka has shown the importance of chain sliding diffusion to crystallization processes and the impact of enhanced axial diffusion in ordered phases. This work is direct quantitative evidence of high axial mobility in the metastable hexagonal phase and extends this phenomenon to crystallization at ambient pressure as performed here.

Chain diffusion between crystalline and amorphous regions in PE, an important dynamic process relevant to polymer transport and viscoelastic properties, was first measured by Schmidt-Rohr and Spiess.[34] These authors used 2D NMR to detect chain translation between different phases of PE, and found enhanced chain diffusivity in the crystalline domains. They demonstrate that even at high molecular weights, PE chain jump processes result in chain diffusion, whereas this

diffusion is hindered in the amorphous phase because of entanglements. The schematic visualization of such motion is shown in Figure 2*c* of Ref. [34], and is similar to what we observe from our simulations (see Figure 5), where large monomer jumps not only are present deep inside ordered domains but entire stems' move during these jumps. Figures 5*a* and *b* show the parallel and perpendicular projection of an ordered domain identified from our simulation at 50 *ns*. Figure *5c* shows a cross section of the system where the monomers are colored by the magnitude of their displacements over an 80 *ps* span. These figures also illustrate the heterogeneous nature of the dynamics inside the ordered domains which is somewhat counterintuitive since it is reasonable to think of ordered domains as regions of low mobility, e.g., in a perfect crystal molecules vibrate around their equilibrium position but usually experience large energy barriers to permanent displacement from equilibrium. This motional heterogeneity is a general feature throughout the entire 100 *ns* simulation. Furthermore, the positions of stems with high and low mobility appear uncorrelated inside the domain, whereas one might expect stems near the surface of a domain to exhibit higher mobility.

To further quantify the heterogeneous large-scale atomic segment (stem) mobility associated with the ordered domains we compute the components of monomer displacement directed parallel and perpendicular to the axial direction of the domains, $D_{\parallel/\perp}(\mathbf{A},\Delta\mathbf{r}(\Delta t))$. These are calculated for a given domain as,

$$D_{\parallel/\perp}(\mathbf{A},\Delta\mathbf{r}(\Delta t)) = \begin{cases} \dfrac{\sum_i^P \left|\mathbf{A}\cdot\Delta\mathbf{r}_i(\Delta t)\right|}{P}, & \parallel \\ \dfrac{\sum_i^P \left|\mathbf{A}\times\Delta\mathbf{r}_i(\Delta t)\right|}{P}, & \perp \end{cases}, \tag{7}$$

where $D_{\parallel/\perp}(\mathbf{A},\Delta\mathbf{r}(\Delta t))$ is the average monomer displacement parallel/perpendicular to the axial direction, $\mathbf{A}$, of an isolated domain, $\Delta\mathbf{r}_i(\Delta t)$ is the displacement of monomer i over Δt, and P is the total number of monomers inside the domain. Also note that the directional velocity, $v(t)$, can be easily obtained from the directional displacement via the following relationship:

$$v_{\parallel/\perp}(t) = \frac{D_{\parallel/\perp}(\mathbf{A},\Delta\mathbf{r}(\Delta t))}{\Delta t}. \tag{8}$$

Figure 6 shows the directional displacement, $D_{\parallel/\perp}(\mathbf{A},\Delta\mathbf{r}(\Delta t))$, parallel (circles) and perpendicular (squares) to the axial direction of the domain as a function of time averaged over the 50 largest domains, as identified at 100 *ns*. The monomers which compose the domains are traced in time from their positions at 0 *ns* to their final positions in the domain at 100 *ns*, and their incremental displacements are calculated every 80 *ps*. Remarkably, the average displacement along the axial direction remains nearly constant whereas the average perpendicular displacement decays with time. The decay in the perpendicular displacement is likely due to the incorporation of monomers into the domain, which limit the overall lateral mobility. Thus, stems become fixed with respect to lateral motion in the domains, leaving chain sliding as the predominant mechanism of mobility, which is virtually unimpeded by further domain formation. The initially high values seen in the lateral displacement maybe due to the "bundling" of stems during the pre-transition period (cluster formation). For monomers in the ordered domains at late times, the displacement per time step along the axial direction is about three times larger than the displacement perpendicular to the axial direction. This is a direct consequence of the structure of the domains, and fits well with the model of weakly-structured stems or 'rods' that pack into well defined hexagonal bundles, that have a propensity to slide by each other relatively easily in the longitudinal (parallel) direction. Such high mobility for chain sliding has broad consequences for the further evolution of the structure. These include the ability to free the physical cross-links between domains, which may provide the necessary degrees of freedom to disentangle chains from the amorphous regions.

Figure 7 qualitatively illustrates the time evolution of a single polymer chain (colored red in the figure) being incorporated into an ordered hexagonal phase domain. The chain-sliding motion, and rapid mobility is apparent. It is seen that as the domain orders over time, the polymer is effectively reeled into the ordering domain. Specifically, during the time period of 20-60 *ns*, the portion of the chain within the amorphous region is rapidly incorporated into the ordered domain, generating stems equal to that of the thickness of the domain in which it is incorporating itself into. Once the chain is incorporated into the domain at ~ 60 *ns*, the chain further anneals itself by eliminating gauche defects and further registers within the domain.

Various theories treat the thermodynamic stability of semicrystalline structures in polymers (e.g., lamellar thickness). It is important to recognize, however, that these structures are metastable, and the kinetics of the crystallization process play an essential role in determining the final structure via processes such as disentanglement of chains at the lamella surface during lamellar thickening or chain sliding during rotation and translation of nuclei. As revealed here, the high longitudinal mobility of the ordered phase facilitates these processes and as such, is vital to the process of crystallization.

Conclusions

These simulations provide new insight into the polymer dynamics during ordering prior to crystallization into well-defined crystalline lamelli. These are the first MD simulations of entangled chains with a box size large enough for several independent lamellar domains to form accessing timescales up to 100 ns. These simulations show the formation of ordered domains thermodynamically distinct from the melt, but with much higher axial monomer mobility than can be expected for the final crystalline phase. In fact, this mobility is similar in magnitude to that of the melt. We note that these results maybe related to the recent observations of mesomorphic phase of Ref.[5], and offer important insights for further understanding of the fundamental principles of the polymer crystallization process.

Acknowledgements

We thank to Prof. Hendrik Meyer for helpful discussion on chain rigidity and torsional potentials for polyethylene. This work performed under the auspices of the U.S. Department of Energy by Lawrence Livermore National Laboratory under Contract DE-AC52-07NA27344.

FIGURE CAPTIONS

Figure 1. The torsional potential (a) used in the present study (dashed) compared to the PYS torsional potential (solid). Population of *trans* and *gauche* states at T = 500 K for the polymer model used in this work (dashed) and the PYS polymer model (solid). The conformer fractions for the model used in this work are $f(t) = 0.80$ and $f(g^{\pm}) = 0.20$, where the conformer fractions for the PYS model are $f(t) = 0.63$ and $f(g^{\pm}) = 0.37$.

Figure 2. Snapshots from the MD simulations showing (*a*) stems at 0 *ns* (note the absence of domains but strong alignment of individual stems. (*b*) 50 largest ordered domains formed at ~ 2 *ns.* (*c*) 50 largest ordered domains isolated at 100 *ns*. (*d*) Single ordered domain consisting of > 60,000 monomers, isolated at 100 *ns.* (e) Amorphous (dark gray) and ordered regions (light gray) isolated at 100 *ns.*

Figure 3. (*a*) Time-dependence of the average number of ordered domains, N_c. (*b*) Average number of particles per ordered domain, N_{pc}. (*c*) Average stem length, $\langle l_s(t) \rangle$. (*d*) Correlation function of axial domain direction, (<|$\mathbf{A}_i \cdot \mathbf{A}_j$|>. Correlation decreases in the time interval 5-10 *ns*. Ordered domains grow in size but they do not order with respect to each other on the timescales of our simulations (<|$\mathbf{A}_i \cdot \mathbf{A}_j$|> saturates after ~ 20 *ns*).

Figure 4. Distribution of monomer energies (non-bonding terms only) at 100 *ns* for the entire system (solid line), an isolated ordered domain at 4 *ns* (dotted line), and isolated ordered domain at 100 *ns* (dot-dashed line), and for the entire system at early (4 *ns,* dashed line).

Figure 5. Parallel (*a*) and perpendicular (*b*) projections of an ordered domain at 50 *ns* consisting of > 60,000 monomers. Monomers with 5% highest displacements are colored black and those with 5% lowest displacements are light gray. Panel (*c*) shows a cross section of the entire ensemble at 100 *ns,* were monomers are shaded according to a their normalized displacement, Δr. Note that entire stems are mobile within this time interval.

Figure 6. Directional displacement, $D_{\parallel/\perp}(\mathbf{A},\Delta\mathbf{r}(\Delta t))$: Average projection of monomer displacement per 80 *ps*, parallel and perpendicular to the domain axial direction. The motion is enhanced in the direction parallel to the domain axial direction, while the monomer motion decreases in the direction perpendicular to the domain axial direction.

Figure 7. Snapshots of the time evolution of the chain-sliding motion of a single polymer chain into an ordered hexagonal phase domain along the entire simulation trajectory at 20 *ns* intervals. A single chain is highlighted in red in the below panels, which shows the transition to the folded state in the ordered domain, other chains in the domain are shown in gray.

FIGURES

Figure 1.

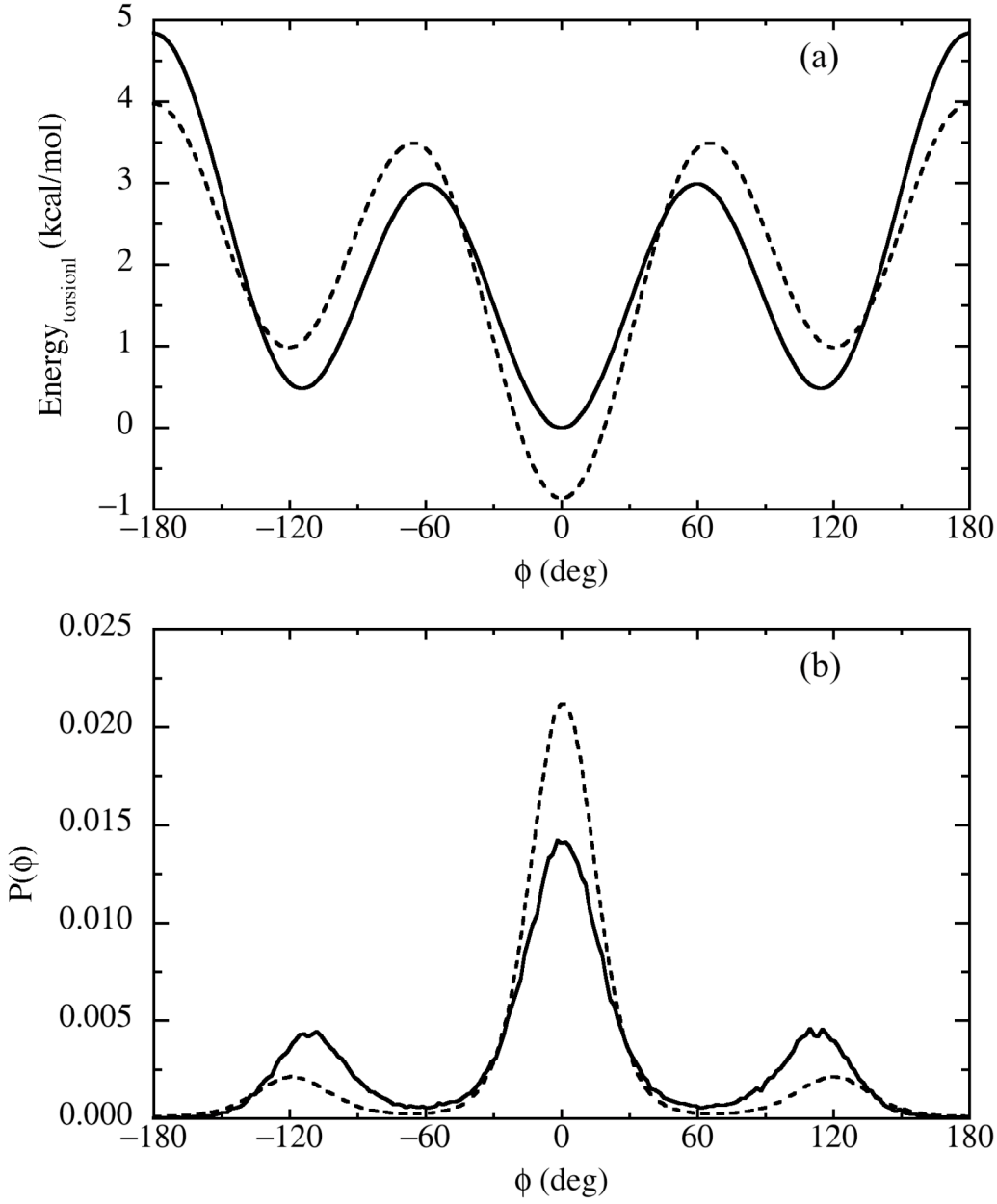

Figure 2.

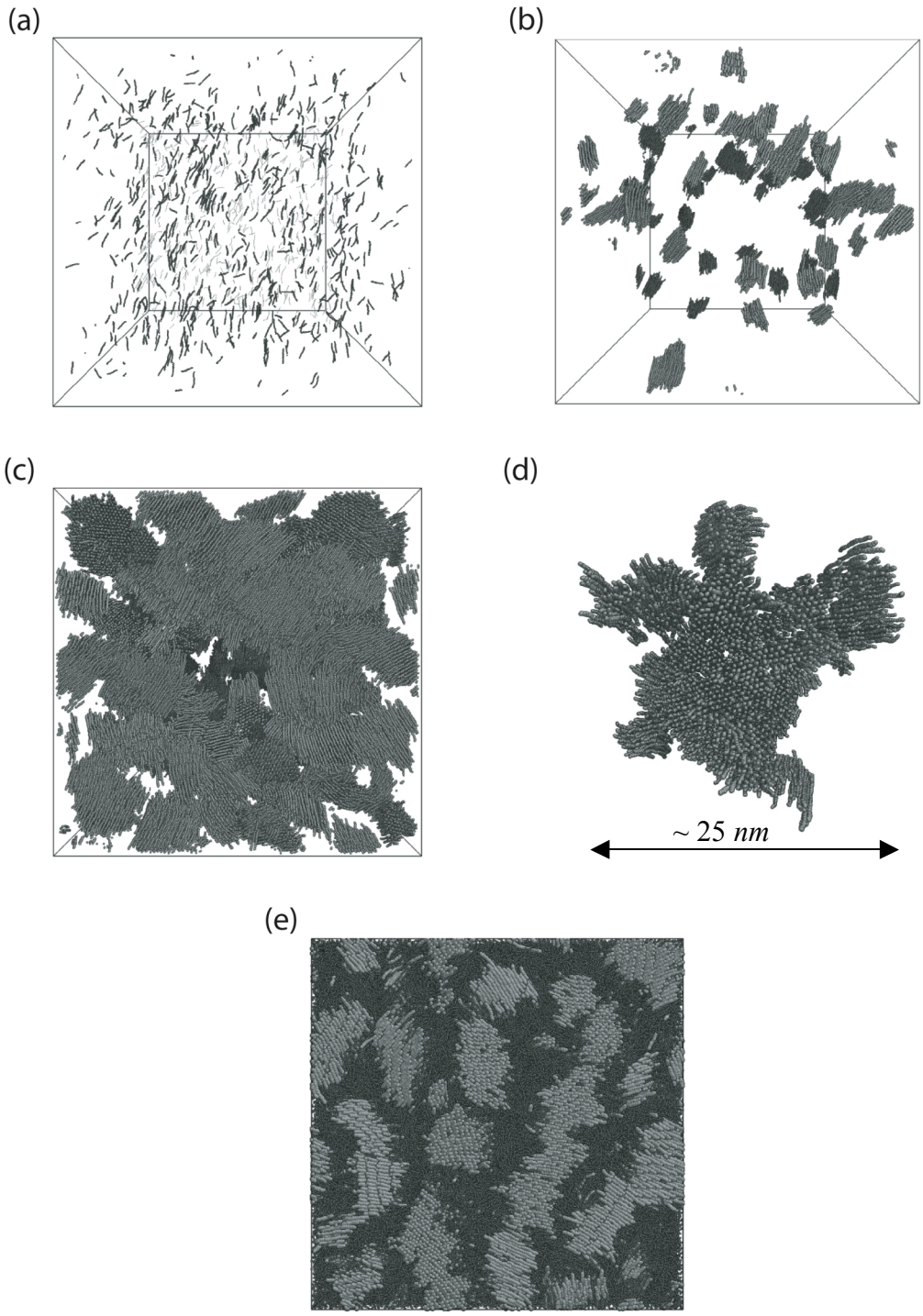

Figure 3.

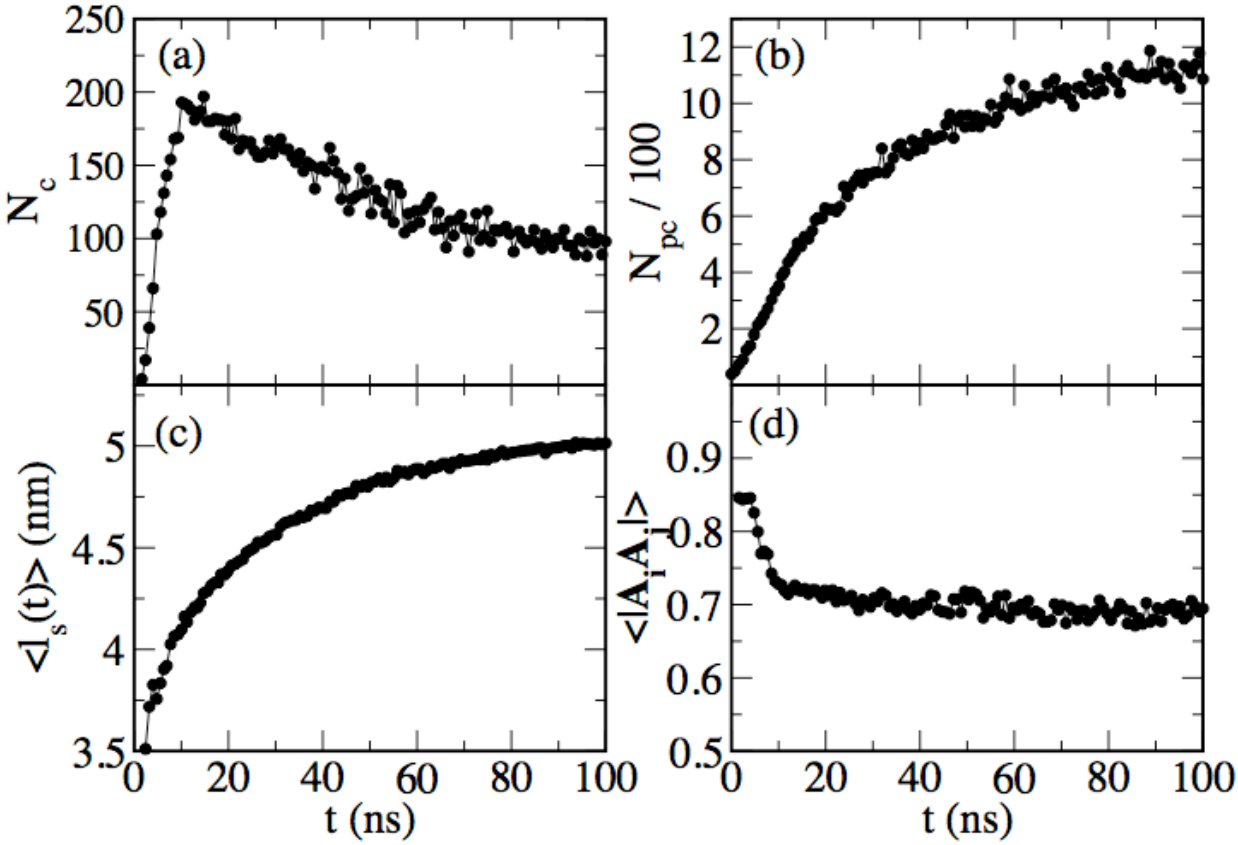
(a)
(b)
(c)
(d)
N_c
N_{pc} / 100
$\langle l_s(t) \rangle$ (nm)
$\langle |A_i A_j| \rangle$
t (ns)
t (ns)

Figure 4.

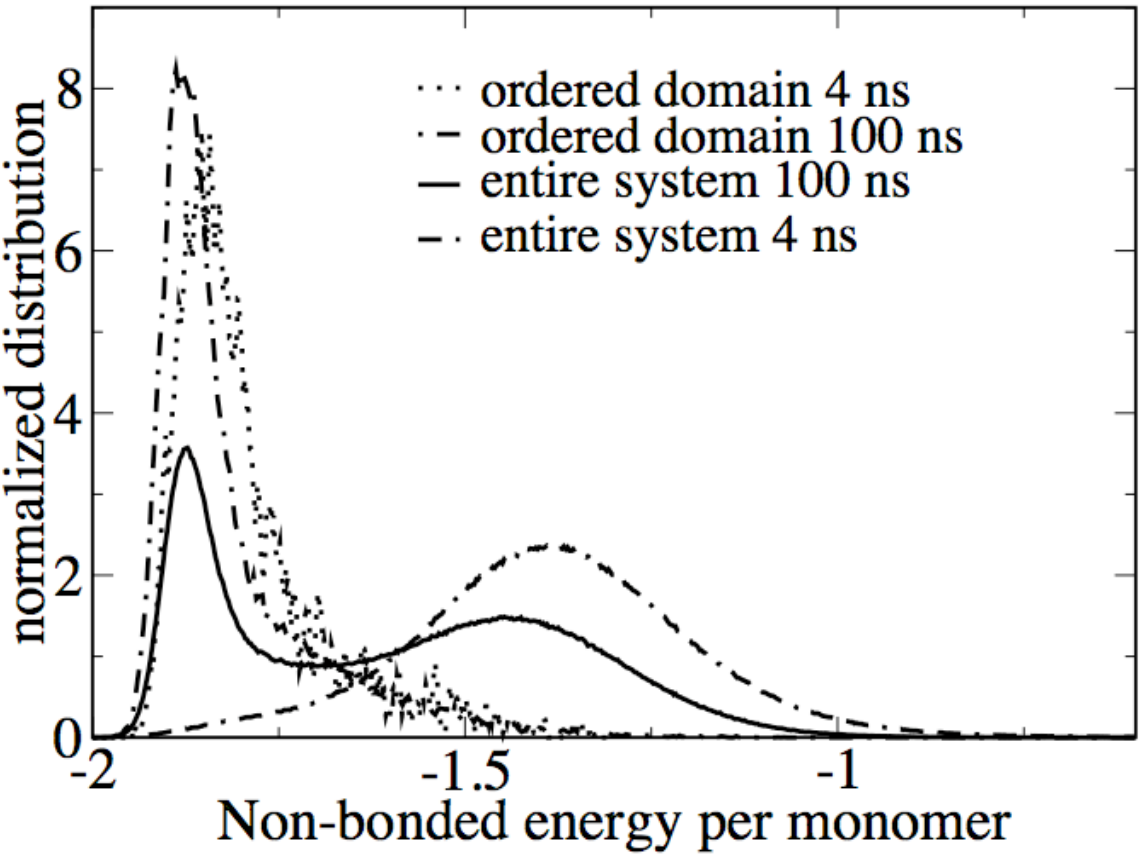
ordered domain 4 ns
ordered domain 100 ns
entire system 100 ns
entire system 4 ns
normalized distribution
0
2
4
6
8
-2
-1.5
-1
Non-bonded energy per monomer

Figure 5.

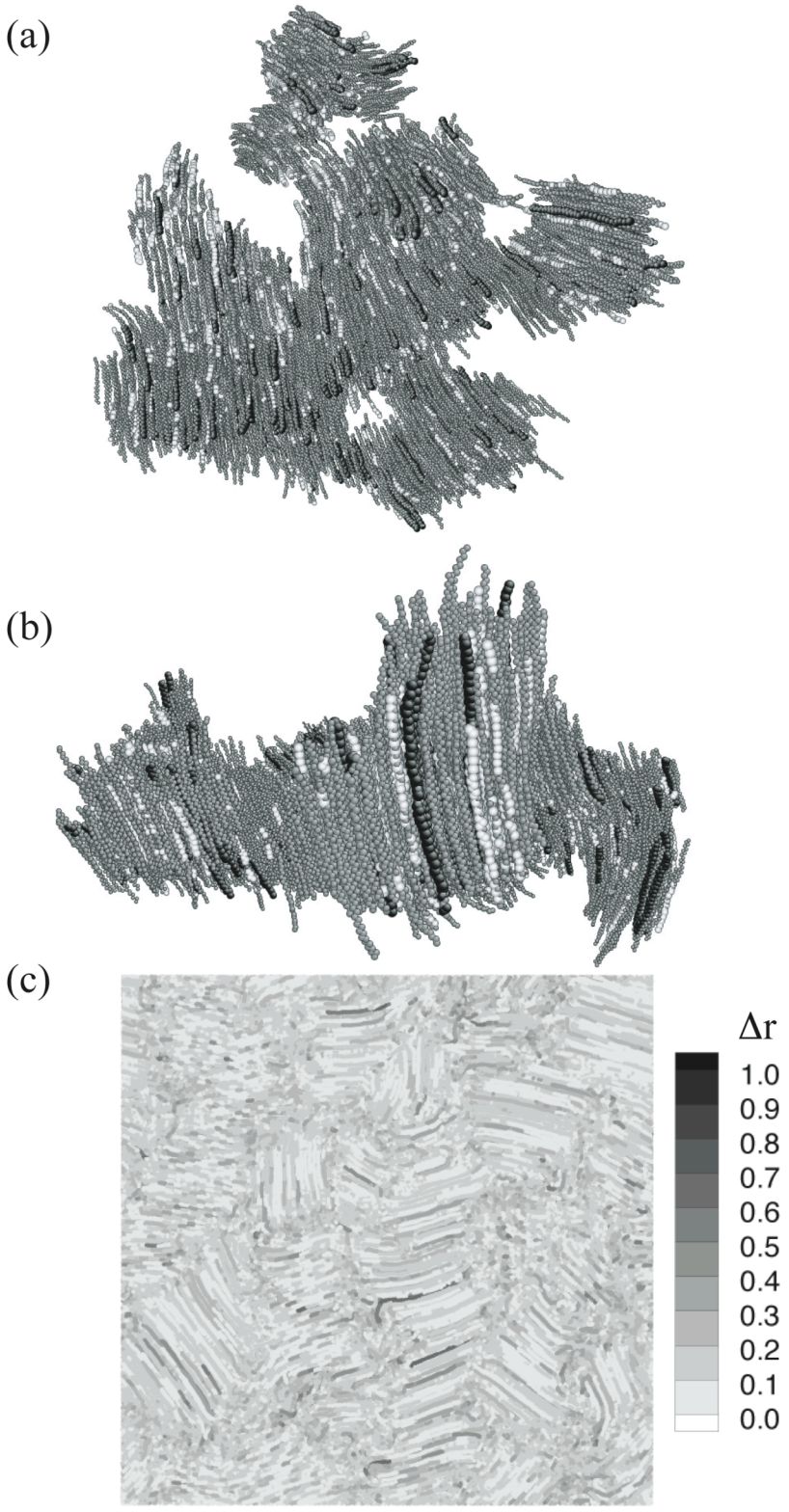

Figure 6.

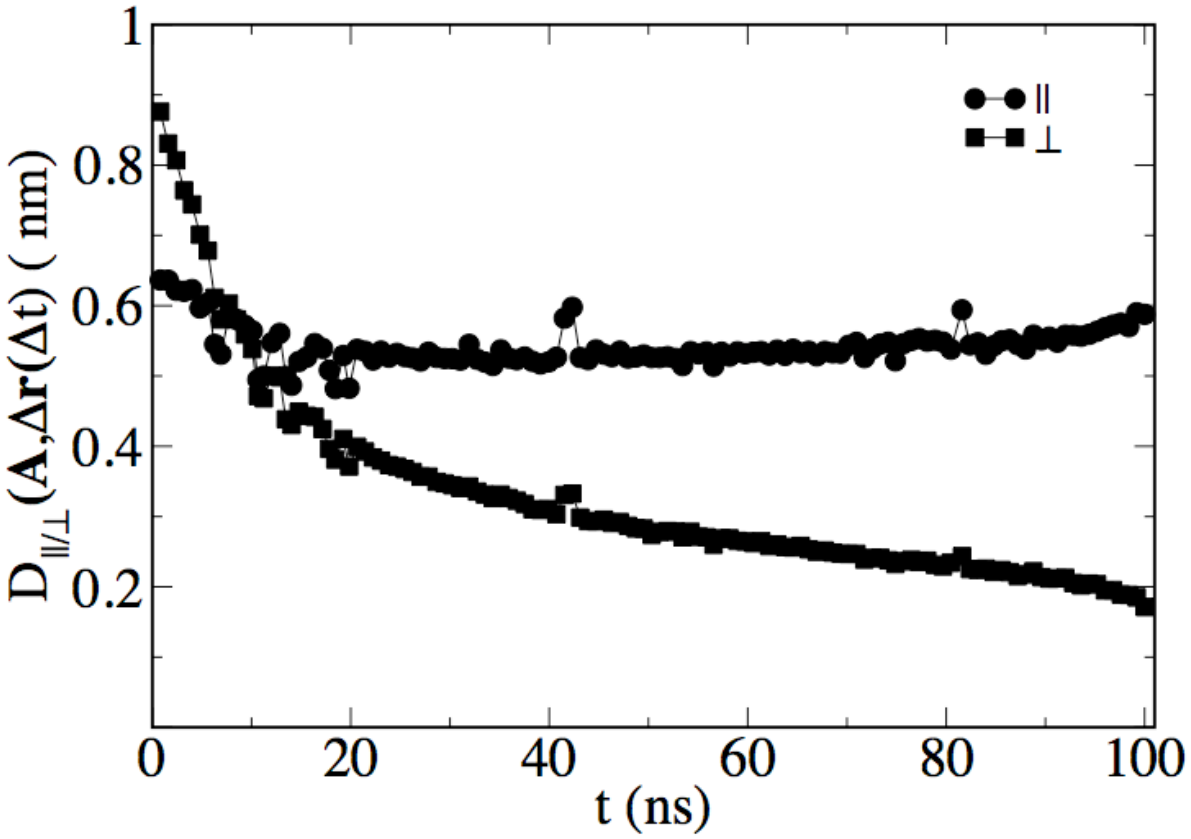

Figure 7.

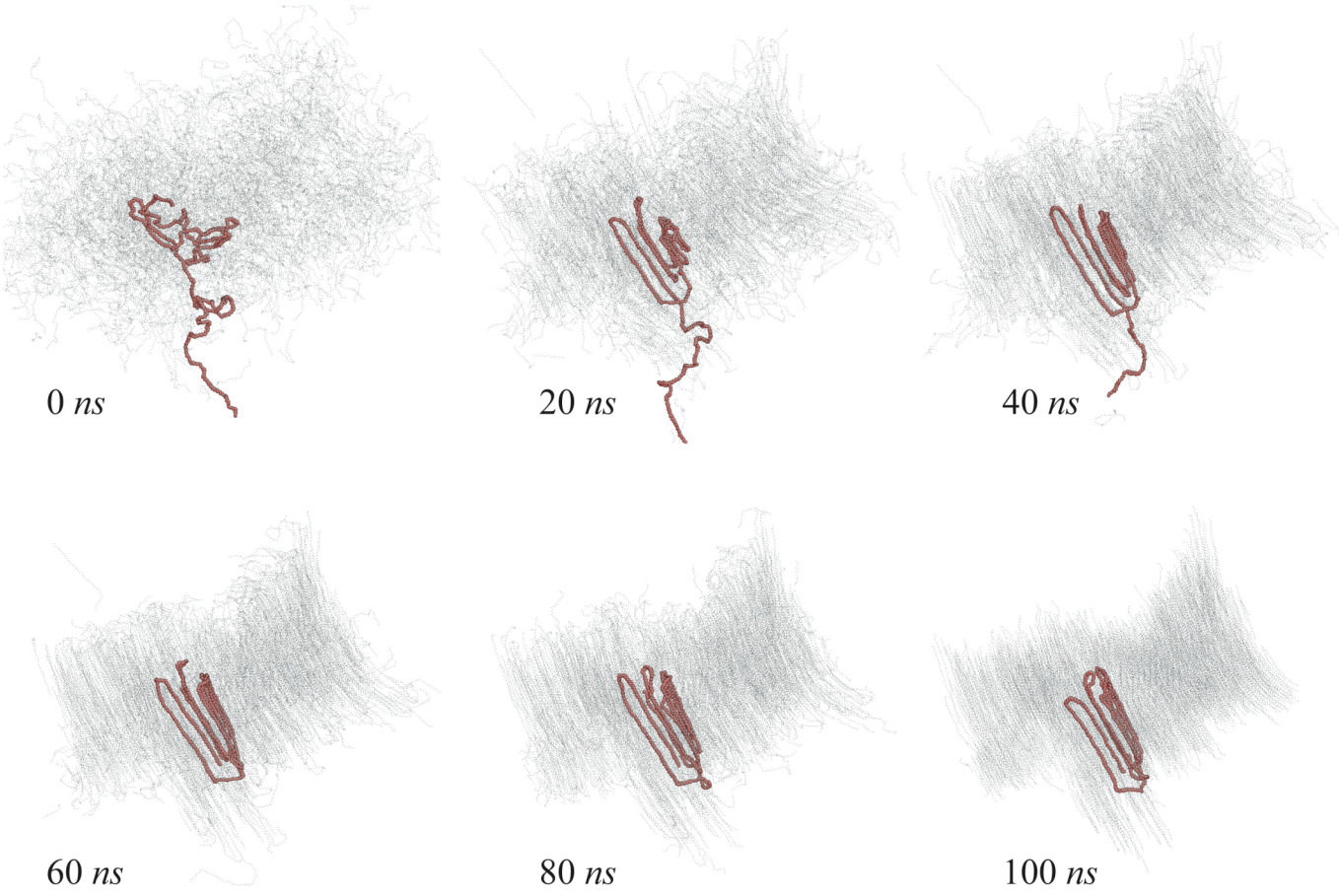

REFERENCES

[1] J. D. Hoffman and J. I. Lauritzen, Journal Of Research Of The National Bureau of Standards A 65 (4), 297 (1961); J. I. Lauritzen and J. D. Hoffman, Journal Of Research Of The National Bureau Of Standards Section A-Physics And Chemistry 64 (1), 73 (1960); J. I. Lauritzen and J. D. Hoffman, Journal of Chemical Physics 31 (6), 1680 (1959).

[2] A. Keller, M. Hikosaka, S. Rastogi, A. Toda, P. J. Barham, and G. Goldbeckwood, Journal of Materials Science 29 (10), 2579 (1994).

[3] M. Imai, K. Kaji, T. Kanaya, and Y. Sakai, Physica B 213&214, 718 (1995).

[4] M. Imai, K. Mori, T. Mizukami, K. Kaji, and T. Kanaya, Polymer 33, 4457 (1992); M. Imai, K. Kaji, and T. Kanaya, Phys. Rev. Lett. 71, 4162 (1993); A. Wurm, R. Soliman, J. G. P. Goossens, W. Bras, and C. Schick, Journal of Non-Crystalline Solids 351 (33-36), 2773 (2005); M. Soccio, A. Nogales, N. Lotti, A. Munari, and T. A. Ezquerra, Physical Review Letters 98 (3) (2007).

[5] G. Strobl, European Physical Journal E 3 (2), 165 (2000).

[6] G. Allegra and S. V. Meille, in *Interphases And Mesophases In Polymer Crystallization Iii* (2005), Vol. 191, pp. 87; P. D. Olmsted, W.C.K.Poon, T. C. B. McLeish, N. J. Terrill, and A.J.Ryan, Physical Review Letters 81 (2), 373 (1998).

[7] R. H. Gee and L. E. Fried, J. Chem. Phys. 118 (8), 3827 (2003).

[8] R. H. Gee, N. Lacevic, and L. E. Fried, Nature Materials 5 (1), 39 (2006).

[9] T. Yamamoto, Journal Of Macromolecular Science-Physics B42 (3-4), 629 (2003).

[10] S. Rastogi, M. Hikosaka, H. Kawabata, and A. Keller, Macromolecules 24 (24), 6384 (1991).

[11] T. Yamamoto, Polymer 45, 1357 (2004).

[12] P. Welch and M. Muthukumar, Physical Review Letters 87 (21), 218302 (2001).

[13] H. Meyer and F. Muller-Plathe, Macromolecules 35 (4), 1241 (2002).

[14] M. Hikosaka, K. Watanabe, K. Okada, and S. Yamazaki, in *Interphases And Mesophases In Polymer Crystallization Iii* (2005), Vol. 191, pp. 137.

[15] M. Imai and K. Kaji, Polymer 47 (15), 5544 (2006).

[16] W. Paul, D. Y. Yoon, and G. D. Smith, J. Chem. Phys. 103 (4), 1702 (1995).

[17] M. Muthukumar and P. Welch, Polymer 41, 8833 (2000).

[18] G. D. Smith, R. L. Jaffe, and D. Y. Yoon, Macromolecules 27, 3166 (1994).

[19] R. H. Gee and R. H. Boyd, Computational And Theoretical Polymer Science 8 (1-2), 93 (1998).

[20] L.-J. Chen, H.-J. Qian, Z.-Y. Lu, Z.-S. Li, and C.-C. Sun, J. Phys. Chem. B 110, 24093 (2006); M. S. Lavine, N. Waheed, and G. C. Rutledge, Polymer 44, 1771 (2003); S. L. Mayo, B. D. Olafson, and W. A. Goddard, J.Phys. Chem. 94, 8897 (1990).

[21] S. J. Plimpton, J. Comp. Phys. 117, 1 (1995).

[22] L. Verlet, Phys. Rev. 159, 98 (1967).

[23] S. Nose, J. Chem. Phys. 81, 511 (1984).

[24] S. Melchionna, G. Ciccotti, and B. L. Holian, Mol. Phys. 78, 533 (1993).

[25] R. H. Boyd and P. J. Phillips, *The Science of Polymer Molecules*, 1st ed. (Cambridge University Press, New York, NY, 1993).

[26] W. L. Mattice and U. W. Sutter, U. W., *Conformational Theory of Large Molecules*. (John Wiley & Sons, New York, 1994).

[27] P. J. Flory, *Statistical Mechanics of Chain Molecules*. (Interscience, New York, 1969).

[28] J. C. Horton, G. L. Squires, A. T. Boothryod, L. J. Fetters, A. R. Rennie, C. J. Glinka, and R. A. Robinson, Macromolecules 22, 681 (1989).

[29] V. Arrighi, J. S. Higgins, R. A. Weiss, and A. L. Cimecioglu, Macromolecules 25 (20), 5297 (1992); H. Kromer, R. Kuhn, H. Pielartzik, W. Siebke, V. Eckhardt, and M. Schmidt, Macromolecules 24 (8), 1950 (1991); G. V. Laivins and D. G. Gray, Macromolecules 18 (9), 1753 (1985).

[30] M. Muthukumar, in *Interphases And Mesophases In Polymer Crystallization III* (2005), Vol. 191, pp. 241.

[31] F. K. a. L. H. Bolz, presented at the Proceedings of the 38th Annual Electron Microscopy Society of America San Francisco, 1980 (unpublished).

[32] M. Hikosaka, Polymer 31 (3), 458 (1990); M. Hikosaka, Polymer 26 (8), 1257 (1987).

[33] R. H. Boyd, Polymer 26, 323 (1985).

[34] K. Schmidt-Rohr and H. W. Spiess, Macromolecules 24 (19), 5288 (1991).